

Lightest and heaviest two-neutron halo nuclei, ${}^6\text{He}$ and ${}^{22}\text{C}$

Waleed S. HWASH*

Department of Physics, Faculty of Education for Pure Sciences, Anbar University, Anbar, Iraq

Received: 26.11.2016

Accepted/Published Online: 21.12.2016

Final Version: 18.04.2017

Abstract: The microscopic cluster model approach has been performed to study the nuclear structure of the lightest and heaviest two-neutron halo nuclei, ${}^6\text{He}$ and ${}^{22}\text{C}$, respectively. The matter radius and binding energy for the ${}^6\text{He}$ and ${}^{22}\text{C}$ nuclei are calculated and the effect of the core deformation (${}^{20}\text{C}$) on the properties of ${}^{22}\text{C}$ nuclei is also discussed. Calculations have shown that the microscopic cluster model provides a good description of binding energy as well as matter radius in comparison to experimental data. The fittings of some parameters such as central potential depth (V_o), empirical constant (r_o), and surface diffuseness value (a) are discussed to find agreement in the results with the available experimental data. The exotic properties of two-neutron halo nuclides ${}^6\text{He}$ and ${}^{22}\text{C}$ such as weak binding energy, abnormal large matter radius, and Borromean system have been confirmed in the present work.

Key words: Halo nuclei, cluster model, nuclear structure, exotic nuclei

1. Introduction

The progress in radioactive nuclear-beam facilities helps to discover new phenomena in nuclear physics such as halo nuclei, where the core nucleus is surrounded by a halo of orbiting protons or neutrons. The halo phenomenon make the nucleus radius abnormally larger than that predicted by the liquid drop models, but with weak binding energy. The known two-neutron halo nuclides currently are ${}^6\text{He}$, ${}^{11}\text{Li}$, ${}^{14}\text{Be}$, ${}^{17}\text{B}$, ${}^{19}\text{B}$, and ${}^{22}\text{C}$. The lightest one is ${}^6\text{He}$ while the heaviest one is ${}^{22}\text{C}$; these are investigated in this work.

The attractive case of the unusual ${}^{22}\text{C}$ nucleus was lately formulated as a two-neutron halo with a ${}^{20}\text{C}$ core within the renormalized zero-range model [1,2]. This investigation allowed us to put some constraints on the separation energy of two-neutron S_{2n} as well as the ${}^{21}\text{C}$ virtual state energy using the recently extracted matter radius of 5.4 ± 0.9 fm [1,3]. The quoted value of $S_{2n}^{(exp)}$ is 0.42 ± 0.94 MeV [1,3].

The radius of ${}^6\text{He}$ was first derived by Tanihata et al. [4,5] to be $r_m = 2.73(3)$ fm. Consecutively, Tostevin and Al-Khalili [6] arrived at a value of $r_m = 2.54(3)$ fm. Later Alkhazov et al. [7] and Neumaier et al. [7–9] found another result for ${}^6\text{He}$, $r_m = 2.45(8)$ fm. The two valence neutrons are found to be bound by a little less than 1 MeV (0.97 MeV) [10].

2. Theoretical aspect

The three-body system is described in terms of the core with valence neutrons.

*Correspondence: waleed973@yahoo.com

The distances between each couple of particles \vec{r}_{jk} and the distance between the mass center of the pair and a third particle are described in the Jacobian coordinates (\vec{x}, \vec{y})

$$\text{where } x = \sqrt{A_{jk}} \vec{r}_{jk} = \sqrt{\frac{A_j A_k}{A_j + A_k}} \vec{r}_{jk} \text{ and } y_i = \sqrt{A_{(jk)i}} \vec{r}_{(jk)i} = \sqrt{\frac{(A_j A_k) A_i}{A_i + A_j + A_k}} \vec{r}_{(jk)i}.$$

The Hamiltonian of the core determines eigenvalues ε_{core} and eigenstates φ_{core}

$$\text{with } \hat{h}_{core}(\xi_{core}) \varphi_{core}(\xi_{core}) = \varepsilon_{core} \varphi_{core}(\xi_{core}). \quad (1)$$

The total wave function is

$$\Psi^{JM}(x, y, \vec{\xi}) = \varphi_{core}(\xi_{core}) \psi(x, y). \quad (2)$$

$\Psi(x, y)$ contains the spin, radial, and angular of the remaining two bodies relative to the core. The hyperspherical is used to convert a two-dimensional differential equation into coupled one-dimensional equations. The Jacobi coordinates (x, y) are converted into the coordinates of the hyperspherical (hyperangle θ and hyperradius ρ) defined as

$$\rho^2 = x^2 + y^2 \text{ and } \theta = \arctan\left(\frac{x}{y}\right).$$

The hyperspherical expansion ‘‘radial and angular wave functions’’ is

$$R_n(\rho) = \frac{\rho^{5/2}}{\rho_o^3} \sqrt{\frac{n!}{(n+5)!}} L_{nlag}^5(z) \exp\left(\frac{-z}{2}\right), \quad (3)$$

where $z = \rho/\rho_o$.

$$\psi_k^{l_x l_y}(\theta) = N_k^{l_x l_y} (\sin \theta)^{l_x} (\cos \theta)^{l_y} P_n^{l_x + \frac{1}{2}, l_y + \frac{1}{2}}(\cos 2\theta) \quad (4)$$

The valence neutrons wave function is

$$\psi_{n,k}^{l_x l_y}(\rho, \theta) = R_n(\rho) \psi_k^{l_x l_y}(\theta), \quad (5)$$

so $\psi(x, y)$ in Eq. (2) is

$$\psi(x, y) = \psi_{n,k}^{l_x l_y}(\rho, \theta)$$

where $L_{nlag}^5(z)$ is associated Laguerre polynomials for the order $nlag = 0, 1, 2, \dots$. $P_n^{l_x + \frac{1}{2}, l_y + \frac{1}{2}}(\cos 2\theta)$ is the Jacobi polynomial. Eq. (3) is a function of (ρ) due to the z dependence on (ρ) with $z = \rho/\rho_o$. Values of ρ and ρ_o are explained later in this section. $n = l_x + 1$ and we assume $nlag = n$. $N_k^{l_x l_y}$ is a normalization coefficient. k is the hyperangular momentum of quantum number $k = l_x + l_y + 2n$ for $(n = 0, 1, 2, \dots)$. The total wave function comes from the wave function of each body in that system. The internal wave function of every neutron is found from solving the Schrödinger equation. More details about the hyperspherical harmonics formalism is presented in [11,12]. The total Hamiltonian, \hat{H} , is

$$\hat{H} = \hat{T} + \hat{h}_{core}(\vec{\xi}) + \hat{V}_{core-n1}(r_{core-n1}, \vec{\xi}) + \hat{V}_{core-n2}(r_{core-n2}, \vec{\xi}) + \hat{V}_{n-n}(r_{n-n}). \quad (6)$$

The Hamiltonian includes the kinetic energy $\hat{T} = \hat{T}_x + \hat{T}_y$, the core Hamiltonian $\hat{h}_{core}(\vec{\xi})$ depends on the interior variables $\vec{\xi}$, and the two-body interactions V_{core-n} and V_{n-n} are for all the pairs of interacting bodies. The potential is considered as the deformed Wood–Saxon potential in addition to a spin–orbit interaction.

The rotational model is expected for the core structure; therefore, the core has been taken as a deformed axially symmetric rotor. In the body-fixed structure the radius of this core deformation is expanded in terms of the spherical harmonic and, for simplicity, the quadruple term has been retained only, as in Eq. (9):

$$\hat{V}_{core-n}(r_{core-n}, \vec{\xi}) = \frac{-V_0}{\left[1 + \exp\left(\frac{r_{core-n} - R(\theta, \varphi)}{a}\right)\right]} + \frac{-\hbar^2}{m^2 c^2} (2l.s) \frac{V_{s.o}}{4r_{core-n}} \frac{d}{dr_{core-n}} \left(\left[1 + \exp\left(\frac{r_{core-n} - R_{so}}{a_{so}}\right)\right]^{-1} \right), \quad (7)$$

$$V_{n-n}(r_{n-n}) = -\frac{\hbar^2}{m^2 c^2} (2l.s) \frac{V_{s.o}}{4r_{n-n}} \frac{d}{dr_{n-n}} \left(\left[1 + \exp\left(\frac{r_{n-n} - R_{so}}{a_{so}}\right)\right]^{-1} \right), \quad (8)$$

with $R = R_0 [1 + \beta_2 Y_{20}(\theta, \phi)]$. (9)

$R_0 = 1.25 A_{core}^{1/3}$, $R_{so} = R$ is assumed, \vec{l} is the orbital momentum operator between a neutron and a core, \vec{s} is the neutron's spin operator, $m = m_\pi$ is the pion mass for practical calculations $\left(\frac{\hbar}{m_\pi}\right)^2 = 2.0 \text{ fm}^2$, β_2 is the core's deformation parameter, and A_{core} is the core mass number. The position of total mass center is:

$$\vec{r}_{CM} = \frac{1}{A} \sum_{i=1}^A \vec{r}_i, \quad (9)$$

$$r_m^2 = \frac{1}{A} \sum_{i=1}^A (\vec{r}_i - \vec{r}_{CM})^2. \quad (10)$$

r_i is the i nucleon position, r_{CM} is mass center, and the (rms) matter radius $\langle r_m^2 \rangle^{1/2}$ of the halo nucleus is $\langle r_m^2 \rangle^{1/2} = \frac{1}{A} [A_{core} \langle r_m^2(core) \rangle + \langle \rho^2 \rangle]$. (12)

The total quadruple moment can be written as $Q = Q_j + Q_c$, where Q is the total quadruple moment composed of Q_j because of the loose neutron and Q_c for the core. Generally $Q_c \gg Q_j$ [13].

$$Q_c = Q' \left[(3\Omega^2/2J^2) - \frac{1}{2} \right] \quad (11)$$

Eq. (11) can be given as

$$Q_c = Q' \frac{J}{2J+3} \left[\frac{3\Omega^2}{J(J+1)} - 1 \right], \quad (12)$$

where J is the total angular momentum, Ω is the projection of j , and Q' can be taken as $Q' = \frac{4}{5} \delta Z R^2$.

Here, Z is the atomic number, R is the nucleus radius calculated before, and δ is associated with the deformation parameter β_2 ($\beta_2 = 2/3(4\pi/5)^{1/2} \delta$) [13].

Eq. (5) describes the valence neutrons' wave function, and ψ in Eq. (2) is the core wave function, calculated depending on shell model. Eq. (2) itself defines a whole wave function of the two-neutron halo system.

The Hamiltonian of the three-body system in Eq. (6) is carried out to calculate the energy of the three-body halo nucleus. The relationship among the three bodies depends on the Wood-Saxon potential as well as spin-orbit interaction as indicated in Eq. (7). Two configurations, the Y-configuration and T-configuration, are used in this study by using Jacobi coordinates. The core is suggested to be deformed (the core of ${}^6\text{He}$ is zero) and is connected with the two neutrons. The bounded states of ${}^6\text{He}$ and ${}^{22}\text{C}$, the binding energy of ${}^6\text{He}$ and ${}^{22}\text{C}$, the matter rms radius of ${}^6\text{He}$ and ${}^{22}\text{C}$, and a deformation of ${}^{20}\text{C}$ are calculated. In Eq. (3), the values of ρ and ρ_o are approximated from the following formulas:

$$\rho_o = \sqrt{j(j+1)} \text{ where } j = l_x + \frac{1}{2},$$

$$\rho = \sqrt{m_j(m_j+1)} \text{ where } m_j = -j, -j+1, \dots, j.$$

The total angular momentum (j) for a halo neutron depends on the core-n radius, and hence using the approximations, ρ and ρ_o are calculated.

In Eq. (9), $Y_{20}(\theta, \phi)$ is taken as

$$Y_{20}(\theta, \varphi) = \frac{1}{4} \sqrt{\frac{5}{\pi}} (3 \cos^2(\theta) - 1).$$

The Wood-Saxon potential is dependent on the core's deformation parameter β_2 through the radius R , Eq. (9). Throughout the present calculation, the spin-orbit interaction was left deformed (with assumption $r_o = 1.25 \text{ fm}$ where $R_o = r_o A^{1/3}$). Radius R_{SO} is assumed equal to R in the whole deformation. The calculations are carried out for the core deformation parameter range of $\beta_2 \in [-0.7, 0.7]$.

3. Results

In the present work, the two-neutron halo structure nuclei have been investigated by using a microscopic cluster model. This approach has been used on other two-neutron halo nuclides such as ${}^{17}\text{B}$, ${}^{11}\text{Li}$, and ${}^{14}\text{Be}$ and has succeeded in describing the three-body system [14,15]. In this work fitting of some parameters to make this model more suitable for a three-body system or a two-neutron halo nuclide was done to see whether the results were in agreement with the experimental data.

The ${}^6\text{He}$ and ${}^{22}\text{C}$ nuclei were considered in this work, since they are considered the lightest and the heaviest two-neutron halo nuclei. We focused on potential depth (V_o), surface diffuseness value (a), and empirical constant (r_o) parameters and fitted them to provide results.

3.1. ${}^{22}\text{C}$ nucleus

The radius and binding energy of ${}^{22}\text{C}$ as a function of deformation are presented in Figure 1 and Figure 2, respectively. ${}^{22}\text{C}$ consists of 6 protons and 16 neutrons. The core of ${}^{22}\text{C}$ is ${}^{20}\text{C}$, which consists of 6 protons and 14 neutrons. According to the shell model, the core (${}^{20}\text{C}$) has four protons placed in the filled $1P_{3/2}$ level and six neutrons in the filled $1d_{5/2}$ level. If ${}^{20}\text{C}$ is assumed spherical and inert, the $1s_{1/2}$, $1p_{1/2}$, $1p_{3/2}$, and $1d_{5/2}$ states are occupied. When core excitation is included, instead of these four states we have more than 11

blocked eigenstates coupled with the ground and excited states of the core. The total angular momentum J of the core is 0^+ , regarding that the core must be spherical and the deformation be zero, but the experimental values have been referred to. However, within this work we want to know if the core has some degree of freedom or not. The experimental values show the two-body system of ^{21}C unbound is extracted. The probabilities of valence neutrons are $1d_{3/2}$, $2s_{1/2}$, and $1f_{7/2}$. To study the properties of the three-body halo nuclei for ^{22}C , the two-body system of ^{21}C treated as the ground energy state for ^{22}C must be understood. The ^{21}C nucleus made of a core and halo neutron placed at a $1d_{3/2}$ state with energy roughly 50 KeV, $1d_{5/2}$ resonant state, or d-resonance is expected to be about 500 KeV and there is no sure evidence for a d-state; therefore, the d-resonance has been considered. Figure 3 shows the potential variation with deformation, where the potential between the core and a neutron has been affected by deformation. The core-n potential decreases as β_2 increases (for $\beta_2 > 0$) and the core has an oblate shape. Note that the ground energy state of the core ^{20}C is $J^\pi(^{20}\text{C}) = 0^+$. The halo neutron may be coupled with the ground energy state of ^{20}C to produce a nuclear energy state $J^\pi(^{21}\text{C})$, and the halo neutron may also be coupled with the excited energy state of the ^{20}C core. We can imagine two d-resonances be on an inert core $[1d_{5/2} \otimes 0^+]1/2^+$ and also on the excited core $[2s_{1/2} \otimes 2^+]1/2^+$. From Figure 3 the very weakly bound energy is with the higher deformation (the negative side that means ‘‘oblate shape’’) at $\beta_2 < -0.4$, suggesting that the halo neutron built on the excited core may not be entirely accurate. However, that is not our goal.

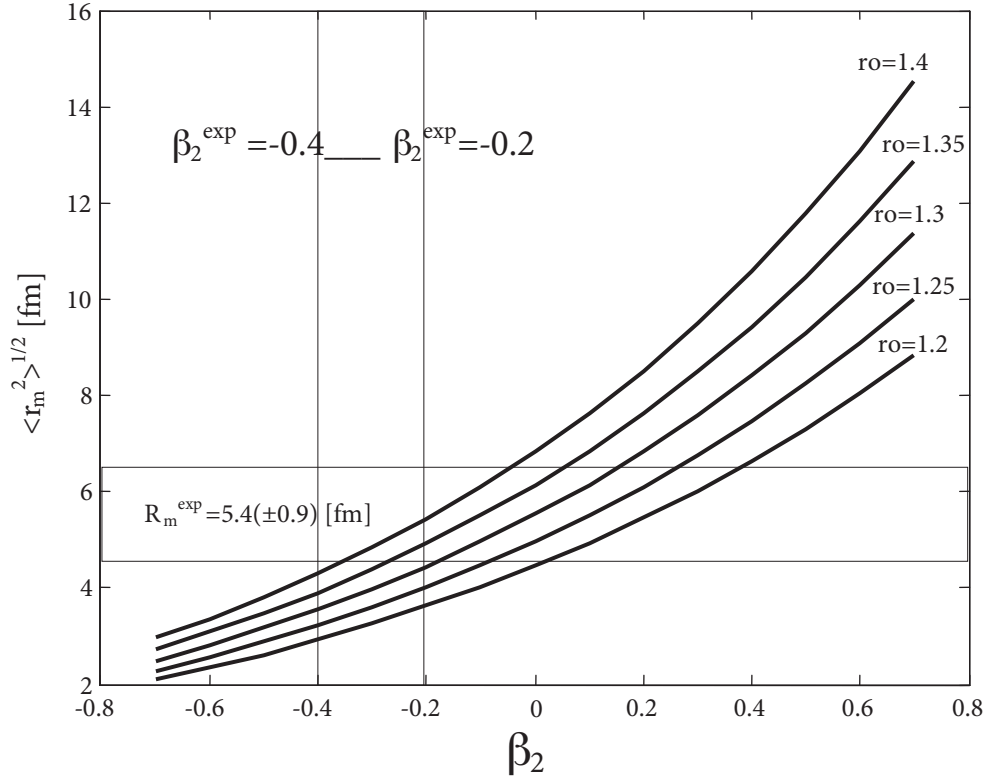


Figure 1. The rms matter radius of ^{22}C as a function of deformation.

As seen in Figure 1, the empirical constant r_o changes from 1.2 to 1.4 fm, indicating that $r_o = 1.4$ fm is more suitable to calculate matter radius and corresponds with the experimental core deformation parameter

and experimental matter radius. This value has been used to calculate the binding energy of ^{22}C with some changes in values of potential depth, V_o , and surface diffuseness, a . In Figure 2, the potential depth changed from $V_o = 50$ to $V_o = 90$ MeV. Of course there are some exaggerations in values of $V_o = 80$ and $V_o = 90$ MeV, but even with the exaggerations the results are still far from the experimental value. However, the surface diffuseness has also been changed from a value of $a = 0.50$ to $a = 0.80$ as seen in Figure 3.

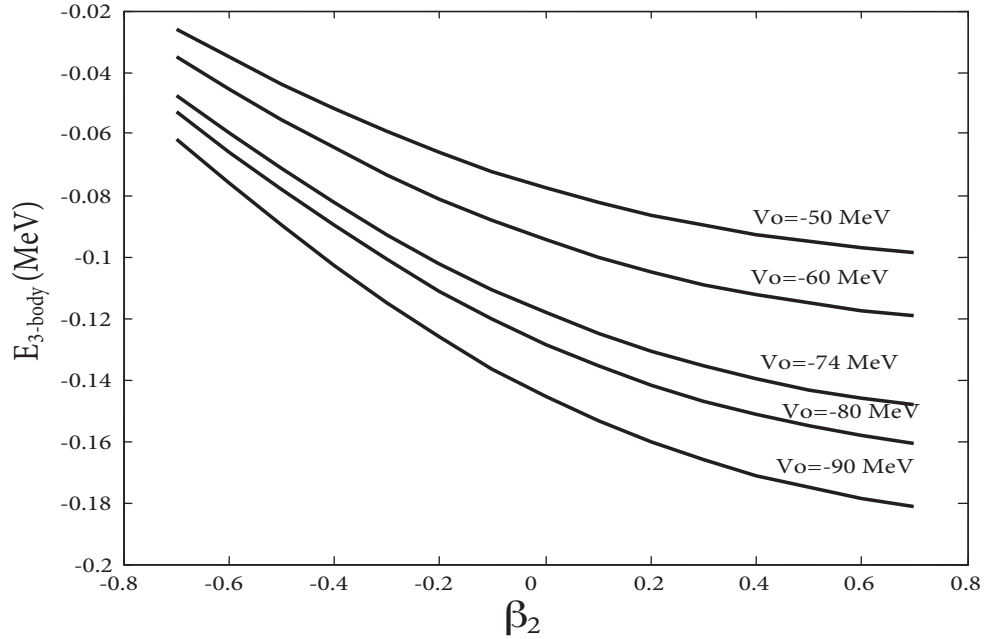


Figure 2. Binding energy of ^{22}C as a function of deformation.

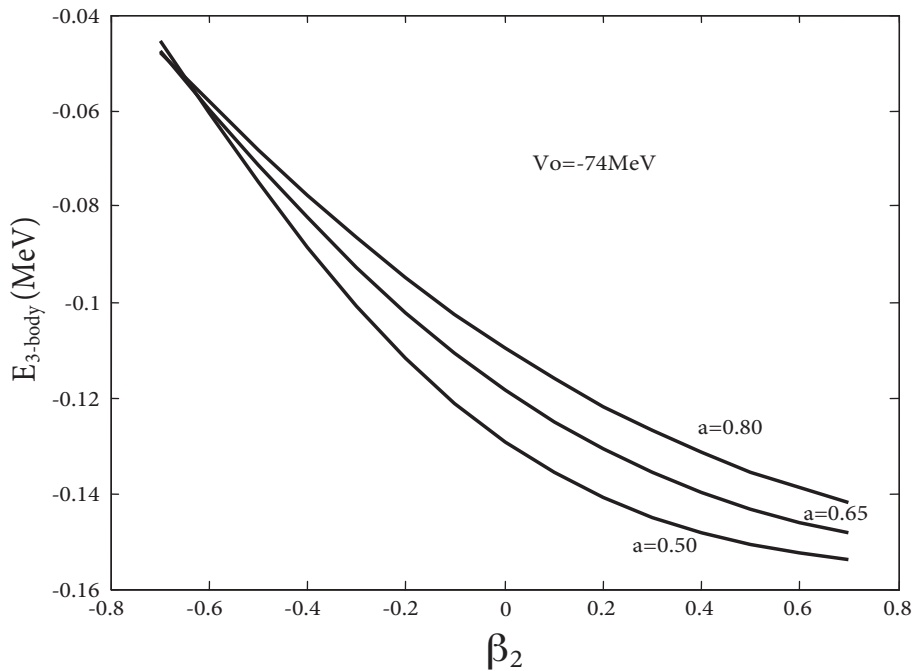


Figure 3. Binding energy of ^{22}C as a function of deformation.

The results in Figures 2 and 3 with all the fittings indicate that the binding energy is less than the experimental value and changing of those parameters does not makes a big difference in the value of the binding energy.

3.2. ${}^6\text{He}$ nucleus

${}^6\text{He}$ consists of four neutrons and two protons, meaning that a core in ${}^6\text{He}$ consists of two protons and two neutrons that occupy the first closed shell and as such the deformation in the core is excluded in this case. Now we have an alpha particle with two valence neutrons, which probably occupy one of the $1p_{1/2}$, $1d_{5/2}$, and $1d_{3/2}$ states. The $1p_{3/2}$ state is excluded because if the valence neutrons occupy $1p_{3/2}$, then ${}^6\text{He}$ is not a halo nucleus and is therefore excluded. The total angular momentum J of ${}^6\text{He}$ equals 0^+ . The aim here is to get a good fitting for the parameters V_o , r_o , and a . The value of the empirical constant r_o is 1.25 ± 0.2 fm and, as seen in Figure 4, $r_o = 1.4$ fm gives a good matter radius of ${}^6\text{He}$ (2.584 fm), which is in agreement with the experimental data. The same value was used to find the binding energy with the value of potential depth V_o from Figure 5, where $r_o = 1.4$ fm and $V_o = 60$ MeV, giving us a good binding energy value of about -1.0237 .

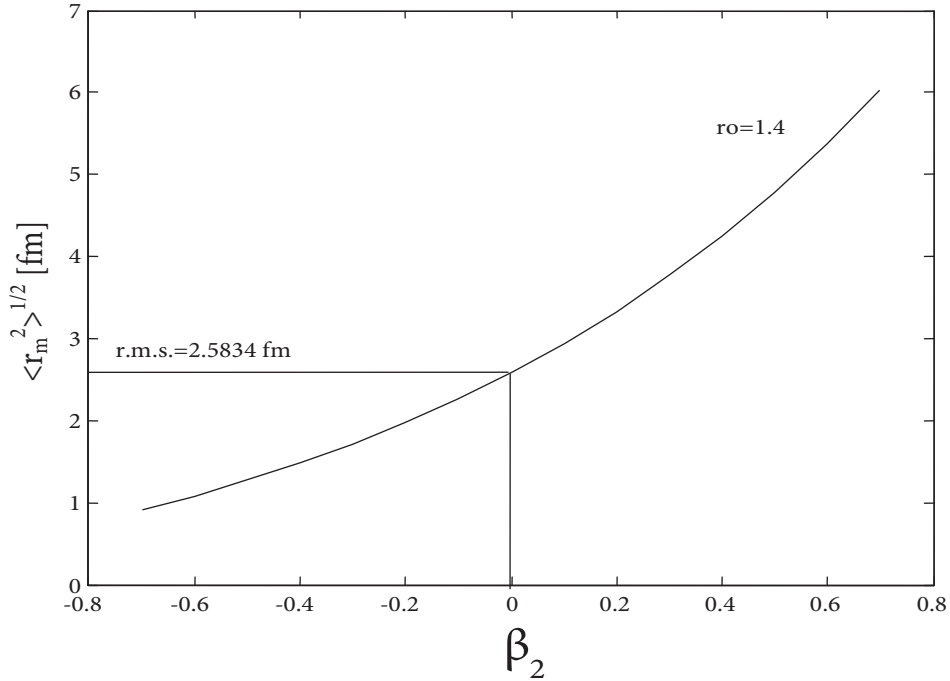


Figure 4. The rms matter radius of ${}^6\text{He}$.

4. Conclusion

The main purpose of the present study is to confirm that the microscopic cluster model is able to describe and calculate the properties of the three-body system (two-neutron halo nuclides) in both the lightest and heaviest two-neutron halo nuclei. As a conclusion, the use of the microscopic cluster model is successful in explaining the properties of the lightest and heaviest two-neutron halo nuclei of ${}^6\text{He}$ and ${}^{22}\text{C}$.

The second purpose is the fitting of parameters such as V_o and r_o in improving this model for accurate calculation of those properties. However, we found that reasonably changing the parameter values only makes

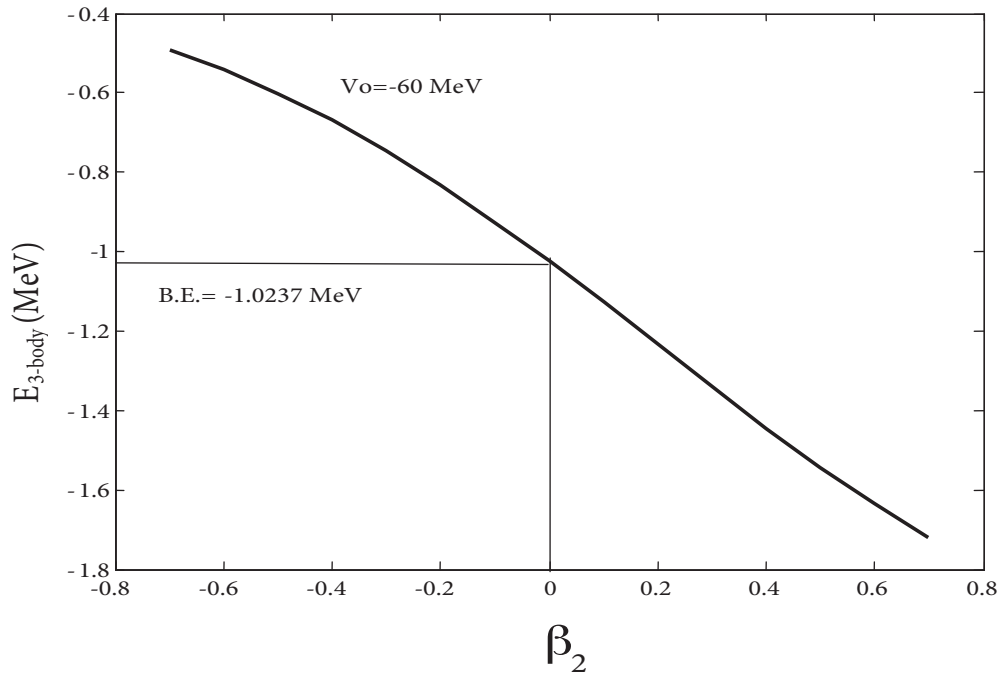


Figure 5. Binding energy of ${}^6\text{He}$ as a function of deformation.

small differences in the results and the values of $V_o = 60$ MeV, $r_o = 1.4$ fm, and $a = 0.5$ give good results in comparison to the experimental data. There were two possibilities, to build the valence neutron (halo neutron) on the excited core or on the inert core, but the results showed that a neutron built on the excited core is not totally accurate.

As seen from the figures, the results of ${}^6\text{He}$ are more in agreement with the experimental data than those of ${}^{22}\text{C}$. This may be due to the number of protons, which has an effect on the total potential by Coulomb repulsion. The core deformation has an effect on the results. The core deformation of ${}^6\text{He}$ is zero, but for ${}^{20}\text{C}$ it has a value of about ($\beta_2 = -0.4$ – $\beta_2 = -0.2$), which could be considered for further studies.

References

- [1] Frederico, T.; Delfino, A.; Tomio, L.; Yamashita, M. *Prog. Part. Nucl. Phys.* **2012**, *67*, 939-994.
- [2] Yamashita, M.; Marques, R.; Frederico, T.; Tomio, L. *Phys. Lett. B* **2011**, *697*, 90-93.
- [3] Tanaka, K.; Yamaguchi, T.; Suzuki, T.; Ohtsubo, T.; Fukuda, M.; Nishimura, D.; Takechi, M.; Ogata, K.; Ozawa, A.; Izumikawa, T. et al. *Phys. Rev. Lett.* **2010**, *104*, 062701.
- [4] Tanihata, I.; Hamagaki, H.; Hashimoto, O.; Nagamiya, S.; Shida, Y.; Yoshikawa, N.; Yamakawa, O.; Sugimoto, K.; Kobayashi, T.; Greiner, D. et al. *Phys. Lett. B* **1985**, *160*, 380-384.
- [5] Tanihata, I.; Hamagaki, H.; Hashimoto, O.; Shida, Y.; Yoshikawa, N.; Sugimoto, K.; Yamakawa, O.; Kobayashi, T.; Takahashi, N. *Phys. Rev. Lett.* **1985**, *55*, 2676.
- [6] Tostevin, J.; Al-Khalili, J. *Nucl. Phys. A* **1997**, *616*, 418-425.
- [7] Alkhazov, G. D.; Andronenko, M. N.; Dobrovolsky, A. V.; Egelhof, P.; Gavrillov, G. E.; Geissel, H.; Irnich, H.; Khazadeev, A. V.; Korolev, G. A.; Lobodenko, A. A. et al. *Phys. Rev. Lett.* **1997**, *78*, 2313-2316.
- [8] Neumaier, S. R.; Alkhazov, G. D.; Andronenko, M. N.; Dobrovolsky, A. V.; Egelhof, P.; Gavrillov, G. E.; Geissel, H.; Irnich, H.; Khazadeev, A. V.; Korolev, G. A. et al. *Nucl. Phys. A* **2002**, *712*, 247-268.

- [9] Alkhazov, G. D.; Dobrovolsky, A. V.; Egelhof, P.; Geissel, H.; Irnich, H.; Khanzadeev, A. V.; Korolev, G. A.; Lobodenko, A. A.; Münzenberg, G.; Mutterer, M. et al. *Nucl. Phys. A* **2002**, *712*, 269-299.
- [10] Sherr, R. *Phys. Rev. C* **1996**, *54*, 1177-1181.
- [11] Nunes, F. M.; Christley, J. A.; Thompson, I. J.; Johnson, R. C.; Efros, V. D. *Nucl. Phys. A* **1996**, *609*, 43-73.
- [12] Tarutina, T.; Thompson, I.; Tostevin, J. A. *Nucl. Phys. A* **2004**, *733*, 53-66.
- [13] Hornyak, W. *Nuclear Structure*; Elsevier Science & Technology Books: Amsterdam, the Netherlands, 1975.
- [14] Hwash, W. S.; Yahaya, R.; Radiman, S.; Ismail, F. *Int. J. Mod. Phys. E* **2012**, *21*, 1250066.
- [15] Hwash, W. S.; Yahaya, R.; Radiman, S. *Phys. Atom. Nucl.* **2014**, *77*, 275-281.